Nuclear envelope defects cause stem cell dysfunction in premature-aging mice

Jesús Espada,[1] Ignacio Varela,[1] Ignacio Flores,[2] Alejandro P. Ugalde,[1] Juan Cadiñanos,[1] Alberto M. Pendás,[1] Colin L. Stewart,[3] Karl Tryggvason,[4] María A. Blasco,[2] José M.P. Freije,[1] and Carlos López-Otín[1]

[1]Departamento de Bioquímica y Biología Molecular, Facultad de Medicina, Instituto Universitario de Oncología, Universidad de Oviedo, 33006 Oviedo, Spain
[2]Telomeres and Telomerase Group, Molecular Oncology Program, Spanish National Cancer Research Center, 28029 Madrid, Spain
[3]National Cancer Institute, Frederick, MD 21702
[4]Division of Matrix Biology, Department of Biochemistry and Biophysics, Karolinska Institutet, SE-171 77 Stockholm, Sweden

<div style="writing-mode: vertical">THE JOURNAL OF CELL BIOLOGY</div>

Nuclear lamina alterations occur in physiological aging and in premature aging syndromes. Because aging is also associated with abnormal stem cell homeostasis, we hypothesize that nuclear envelope alterations could have an important impact on stem cell compartments. To evaluate this hypothesis, we examined the number and functional competence of stem cells in *Zmpste24*-null progeroid mice, which exhibit nuclear lamina defects. We show that *Zmpste24* deficiency causes an alteration in the number and proliferative capacity of epidermal stem cells. These changes are associated with an aberrant nuclear architecture of bulge cells and an increase in apoptosis of their supporting cells in the hair bulb region. These alterations are rescued in *Zmpste24*$^{-/-}$ *Lmna*$^{+/-}$ mutant mice, which do not manifest progeroid symptoms. We also report that molecular signaling pathways implicated in the regulation of stem cell behavior, such as Wnt and microphthalmia transcription factor, are altered in *Zmpste24*$^{-/-}$ mice. These findings establish a link between age-related nuclear envelope defects and stem cell dysfunction.

Introduction

Aging is an extremely complex process whose molecular basis remains largely unknown (Kirkwood, 2005). The identification of several molecular mechanisms contributing to aging has been facilitated by studies on premature aging syndromes that lead to the rapid development of many age-related phenotypes (Kipling et al., 2004; Ramirez et al., 2007). Although most of the genes mutated in progeroid conditions encode DNA repair proteins, recent studies have revealed that alterations in other processes such as nuclear envelope formation and dynamics are involved in the development of premature aging syndromes (Hasty et al., 2003; Cadiñanos et al., 2005; Broers et al., 2006). Thus, mice with mutations in lamin A (a major component of the nuclear envelope) or deficient in Zmpste24/Face1 (a metalloprotease involved in pre–lamin A processing) exhibit many features of premature aging (Pendás et al., 2002). Analogously, patients with Hutchinson-Gilford progeria or other progeroid syndromes have mutations in *LMNA* or *ZMPSTE24* genes (Capell and Collins, 2006; Navarro et al., 2006; Ramirez et al., 2007). The relevance of nuclear envelope alterations to the process of aging has been further confirmed after the finding of lamin A–dependent nuclear defects in human physiological aging (Scaffidi and Misteli, 2006). As aging has also been correlated with changes in the number and functional competence of tissue stem cells (Campisi, 2005; Rando, 2006), we hypothesized that the nuclear envelope alterations linked to aging phenotypes could have an important impact on the stem cell compartment. To evaluate this hypothesis, we have used *Zmpste24*-null mice showing nuclear lamina defects and accelerated aging to perform an analysis of putative dysfunctions in their stem cells. We have focused our study on the telogen hair follicle, which contains multipotent stem cells of both epidermal and neural origin located in the bulge region, a niche in the upper hair follicle (Fig. 1, A–C).

Supplemental Material can be found at:
http://jcb.rupress.org/content/suppl/2008/04/07/jcb.200801096.DC2.html
http://jcb.rupress.org/content/suppl/2008/03/31/jcb.200801096.DC1.html

Figure 1. **Zmpste24 deficiency promotes stem cell number alterations in mouse skin.** (A) Schematic representation of the hair follicle indicating the bulge region where epidermal stem cells are contained. (B and C) Distribution of cytokeratin 15 and α6-integrin in the hair follicle of control and *Zmpste24*-null animals. (B) Boxed areas are magnified in the bottom panels. (D) Localization and quantification of LRCs in the hair follicle of the indicated mice. **, P < 0.01. Error bars represent SEM. Bars: (B, top; C and D) 100 μm; (B, bottom) 60 μm.

Results and discussion

To visualize bulge stem cells, we used a labeling technique involving repeated injections of BrdU followed by a long chase period that allows the detection of label-retaining cells (LRCs), which are long-term residents and infrequently cycling cells of adult mouse epidermis (Cotsarelis et al., 1990). As shown in Fig. 1 D, we observed a significant increase in the number of LRCs present in the bulge region of *Zmpste24*$^{-/-}$ mice when compared with those detected in control mice. In contrast, the observed LRC alterations were abolished in *Zmpste24*$^{-/-}$ *Lmna*$^{+/-}$ mice, which do not accumulate pre–lamin A in the nuclear envelope and exhibit a total recovery of the progeroid phenotypes characteristic of *Zmpste24*-null mice (Fig. 1 D; Fong et al., 2004; Varela et al., 2005). As a complementary approach to LRC detection, we performed immunohistochemical studies of cytokeratin 15

and 19 and α6-integrin, which are markers of epithelial stem cells (Liu et al., 2003; Blanpain and Fuchs, 2006). In all cases, and in agreement with the LRC-based experiments, we observed an increased immunoreactive signal in the bulge region from *Zmpste24*-null mice (Fig. 1, B and C; and Fig. S1, available at http://www.jcb.org/cgi/content/full/jcb.200801096/DC1).

To evaluate the possibility that the accumulation of stem cells observed in *Zmpste24*$^{-/-}$ mice could be linked to the nuclear architecture alterations previously described in non–stem cells of these mutant mice (Pendás et al., 2002), we examined the nuclear morphology and distribution of heterochromatic and methylated DNA (5-methylcytosine [5mC]) in the epidermis by using confocal microscopy and immunostaining (Fig. 2 A). We observed profound alterations in the nuclear architecture of the *Zmpste24*$^{-/-}$ hair bulb and interfollicular epithelium cells, which exhibit a clear fusion of heterochromatin clusters (chromocenters)
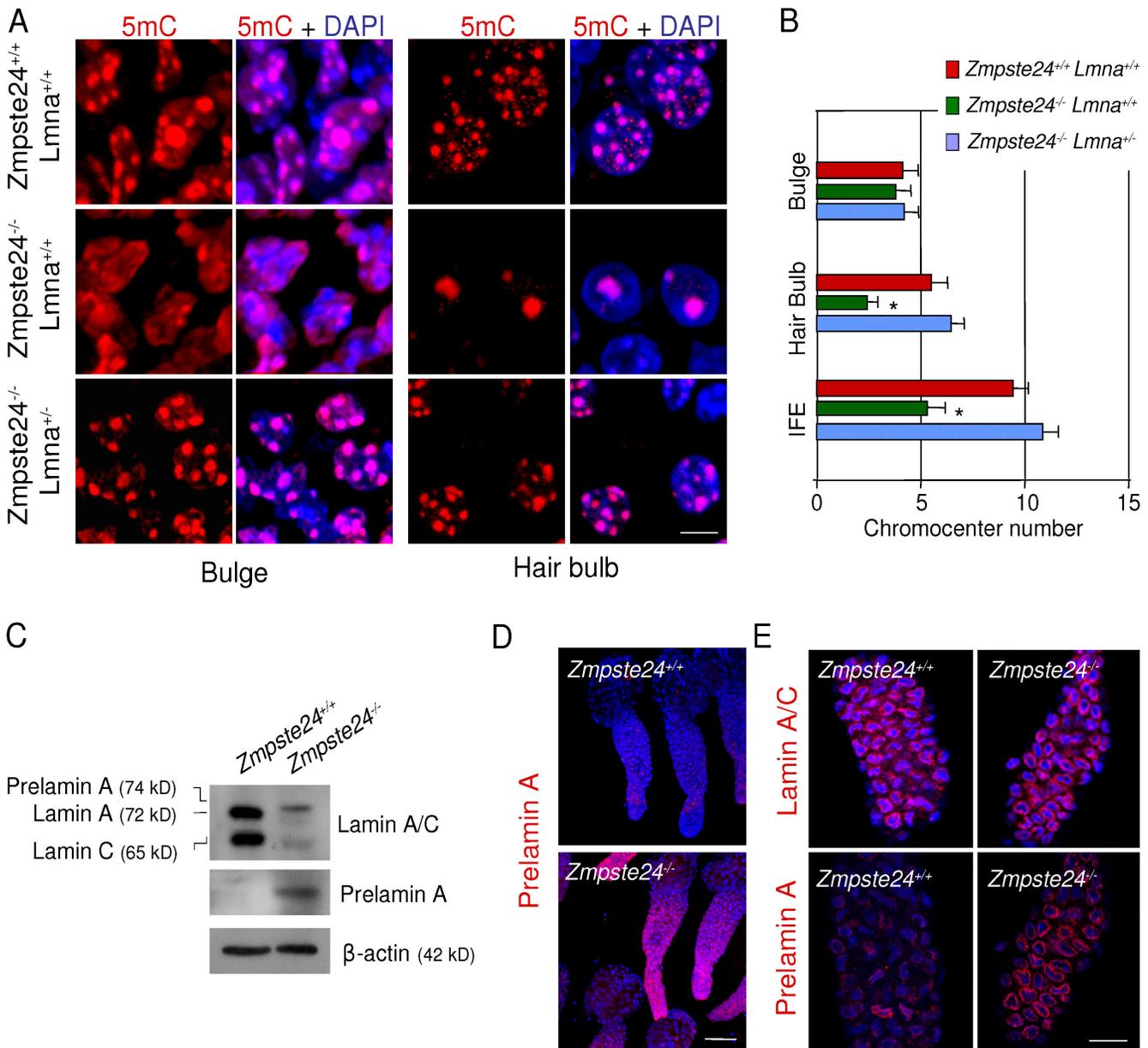
Figure 2. **Nuclear architecture alterations in hair follicle stem cells of *Zmpste24*−/− mice.** (A) Distribution of nuclear heterochromatin and 5mC. (B) Chromocenter quantification in hair follicles from the indicated mice. Cells with nuclear aberrations related to apoptosis were excluded from analysis. 100 cells of each region in three animals per genotype were examined. *, P < 0.05. Error bars represent SEM. (C) Immunoblot analysis of lamin A/C in the epidermis of *Zmpste24*+/+ and *Zmpste24*−/− animals. Results are representative of three different experiments. (D) Immunolocalization of pre–lamin A in tail skin hair follicles from *Zmpste24*+/+ and *Zmpste24*−/− mice. (E) Detailed view of the distribution of lamin A and pre–lamin A in hair follicles from *Zmpste24*+/+ and *Zmpste24*−/− animals. Bars: (A) 10 µm; (D) 100 µm; (E) 50 µm.

and associated 5mC in one or two large masses. In contrast, cells from control mice show numerous chromocenters of small size dispersed in the nucleoplasm and frequently associated with the nuclear envelope (Fig. 2 A; Filesi et al., 2005; Shumaker et al., 2006). Similar gross changes in two heterochromatin markers, HP1α and 3mK9H3, were observed in *Zmpste24*−/− cells (Fig. S2 A, available at http://www.jcb.org/cgi/content/full/jcb.200801096/DC1). Likewise, the determination of chromocenter numbers revealed a significant reduction of heterochromatin clusters in the hair bulb and interfollicular epithelium of *Zmpste24*−/− animals (Fig. 2 B). Furthermore, *Zmpste24*−/− bulge cells show a significant depletion of 5mC, a characteristic

feature of cell senescence (Fig. 2 A; Howard, 1996). Remarkably, these alterations were rescued in *Zmpste24*−/− *Lmna*+/− normal-aging mice (Fig. 2, A and B).

To try to establish a link between stem cell nuclear alterations and the defective lamin A/C processing characteristic of *Zmpste24*−/− animals, we analyzed the expression and distribution of pre–lamin A. An antibody recognizing both pre–lamin A and lamin A/C revealed an increase of pre–lamin A levels in the epidermis of *Zmpste24*−/− animals (Fig. 2 C) and marked the nuclear envelope of bulge stem cells from both *Zmpste24*−/− and *Zmpste24*+/+ mice (Fig. 2, D and E). Furthermore, a pre–lamin A–specific antibody detected this

Figure 3. ***Zmpste24* deficiency reduces the proliferative potential of epidermal stem cells.** (A) Quantification of size and number of macroscopic colonies obtained from isolated epidermal cells purified from skin from newborn and adult mice. (B) Localization of cells undergoing DNA replication by short-term BrdU labeling in hair follicles of the indicated mice treated or not treated with TPA, and quantification of DNA-replicating cells in the bulge region. (C) Detection of cells showing DNA fragmentation by TUNEL assays in hair follicles from the indicated mice, and quantification of TUNEL-positive cells in the hair bulb region of hair follicles treated or not treated with TPA. Boxed areas are magnified in the bottom panels. *, P < 0.05; **, P < 0.01. Error bars represent SEM. Bars: (B and C, top) 100 µm; (C, bottom) 10 µm.

A

B DNA replication

C DNA fragmentation
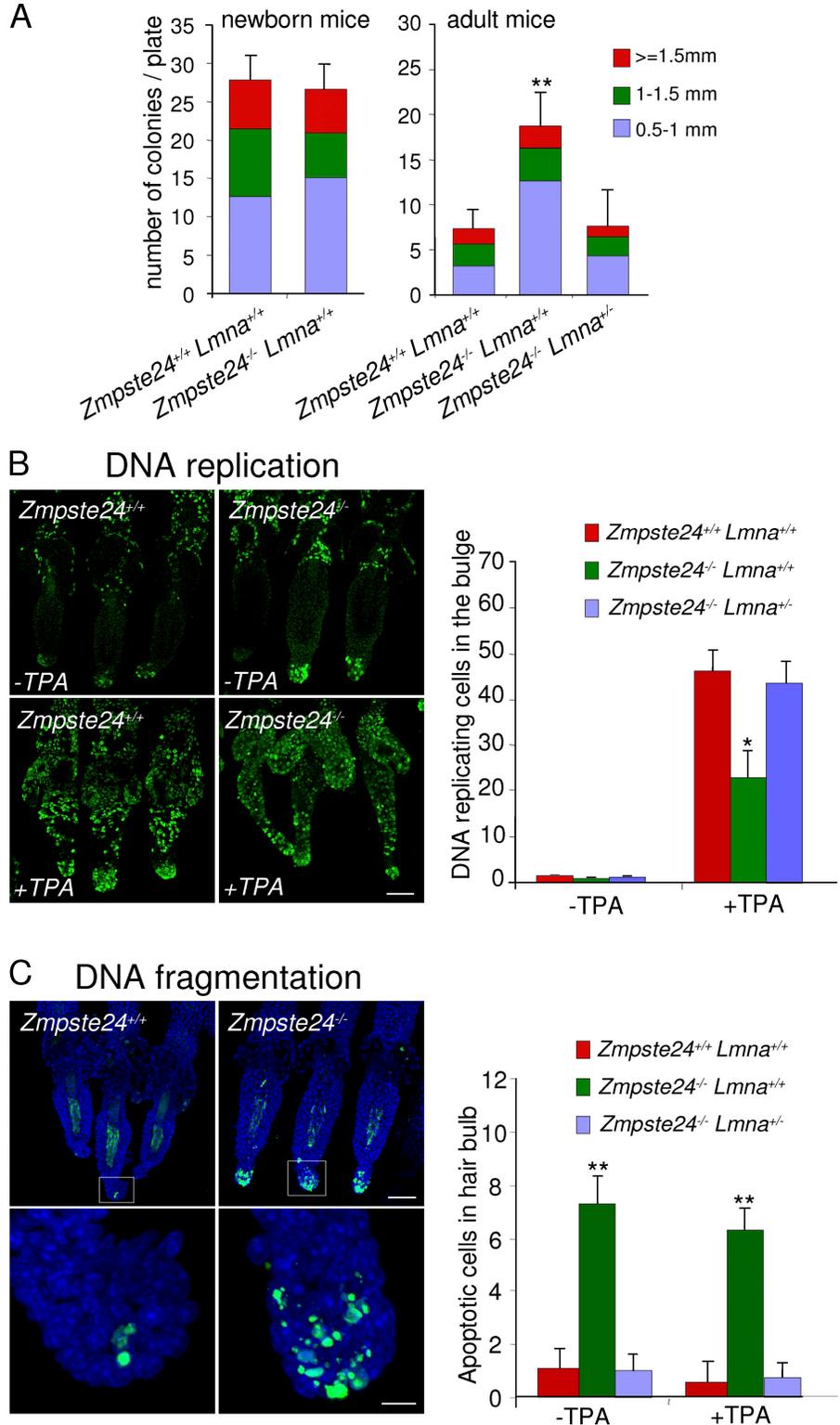
precursor in the epidermis of *Zmpste24*$^{-/-}$ mice (Fig. 2 C). Likewise, a strong accumulation of pre–lamin A in the nuclear envelope of bulge stem cells was observed in *Zmpste24*$^{-/-}$ but not in *Zmpste24*$^{+/+}$ animals (Fig. 2, D and E). According to these results, we conclude that epidermal stem cells from *Zmpste24*-null mice produce and accumulate pre–lamin A in their nuclear envelope, which, in turn, may con-

tribute to the LRC increase and stem cell alterations observed in these progeroid mice.

The observed alterations of epidermal stem cell numbers in *Zmpste24*$^{-/-}$ mice can be initially attributed to a dysfunction in the proliferation or differentiation potential of stem cell reservoirs. To evaluate this question, we first performed clonogenic assays with epidermal cells from newborn and adult *Zmpste24*$^{-/-}$

and *Zmpste24*^{+/+} mice (Fig. 3 A). We did not find significant differences in the clonogenic potential of epidermal cells from newborn mice, which agrees with the notion that *Zmpste24*^{−/−} phenotypic alterations are only detected after several weeks of age (Pendás et al., 2002). In contrast, clear differences were found in the assays performed with epidermal cells from adult mice (Fig. 3 A). Therefore, consistent with the accumulation of LRCs in the bulge region of *Zmpste24*^{−/−} mice, epidermal cells from these mutant animals generated a higher number of colonies than those from control mice. Interestingly, most colonies formed by *Zmpste24*^{−/−} epidermal cells were of small size (between 0.5 and 1 mm; 67% in mutant mice vs. 43% in wild type), suggesting a decreased capacity of *Zmpste24*^{−/−} stem cells to proliferate (Fig. 3 A). The finding that the number and size of colonies obtained from adult *Zmpste24*^{−/−} *Lmna*^{+/−} epidermal cells did not differ from those obtained when wild-type epidermal cells were used confirmed the full rescue of the putative stem cell defects when pre–lamin A levels are lowered.

To further evaluate the observed decline in the proliferative potential of *Zmpste24*^{−/−} stem cells, we investigated the distribution of proliferating cells in the bulge region after treatment with tetradecanoylphorbol 13-acetate (TPA), a tumor promoter that induces the proliferation and differentiation of hair follicle stem cells (Braun et al., 2003). As shown in Fig. 3 B, DNA-replicating cells were absent from the bulge region in both wild-type and *Zmpste24*^{−/−} untreated mice. After TPA treatment, proliferating cells were detected all along the hair follicle in both wild-type and *Zmpste24*^{−/−} animals (Fig. 3 B). However, a significant reduction in the number of DNA-replicating cells was observed in the bulge region of *Zmpste24*^{−/−} animals, indicating the loss of proliferative potential of bulge stem cells from these mutant mice (Fig. 3 B). This proliferative defect was completely rescued in the *Zmpste24*^{−/−} *Lmna*^{+/−} normal-aging mice (Fig. 3 B). To determine whether apoptotic changes could also contribute to the reduced proliferative capacity of stem cells from *Zmpste24*^{−/−} mice, we next analyzed the levels of apoptotic DNA fragmentation in these animals. As shown in Fig. 3 C, we did not find any significant apoptotic changes in the bulge region from *Zmpste24*^{−/−} mice. However, parallel analysis of the hair bulb region that contains the cells responsible for bulge stem cell maintenance and stimulation revealed a strong increase of DNA fragmentation in *Zmpste24*^{−/−} mice (Fig. 3 C). Notably, this apoptosis defect was also rescued in *Zmpste24*^{−/−} *Lmna*^{+/−} mice (Fig. 3 C). We next investigated the potential induction of apoptosis in the hair follicle after the stimulatory signal provided by TPA. As shown in Fig. 3 C, no significant differences in the number and distribution of apoptotic cells were observed in the hair bulb region of *Zmpste24*^{−/−} or their wild-type littermates after TPA treatment. We next tested whether stem cells from *Zmpste24*^{−/−} mice could have changes in their differentiation potential in addition to the observed proliferative deficiencies. However, we failed to observe any difference in the ability of *Zmpste24*^{−/−} or control epidermal stem cells to differentiate into the four epidermal layers after TPA stimulation (Fig. S2 B). Likewise, no changes were observed in the differentiation potential of epidermal keratinocytes subjected to a Ca^{2+} shock, a procedure used to assess stem cell

multipotency (Fig. S2 C; Flores et al., 2005). Nevertheless, we must emphasize that these assays are only qualitative and of limited sensitivity, and further studies will be necessary to assess the occurrence of putative defects in the differentiation potential of *Zmpste24*^{−/−} stem cells.

Taking all of these results into account, we can conclude that the accumulation of LRCs in *Zmpste24*^{−/−} stem cell niches is in part caused by a defect in the proliferation potential of these cells. Moreover, increased apoptosis in the stem cell microenvironment and rapid entry in senescence of a significant proportion of replicating epidermal cells may also contribute to the altered behavior of stem cells in *Zmpste24*^{−/−} mice. Likewise, the finding that these molecular abnormalities occur in both stem cells and their neighboring and supporting cells suggests that *Zmpste24*^{−/−} stem cell dysfunction results from the interplay between cell-intrinsic defects and noncell autonomous changes in their microenvironment. These findings also suggest the possible occurrence of defects in signaling pathways involved in the communication between stem cells and their niches in *Zmpste24*^{−/−} progeroid mice.

Recent studies have provided important information about different signaling pathways involved in the regulation of stem cell functionality (Blanpain and Fuchs, 2006; Clevers, 2006; Jones and Wagers, 2008). Wnt–β-catenin signaling is particularly significant in the context of the observed *Zmpste24*^{−/−} defects because of its relevance to proper stem cell activity during hair follicle morphogenesis in adult mice (Lo Celso et al., 2004; Clevers, 2006). To investigate putative abnormalities in this regulatory pathway in *Zmpste24*^{−/−} mice, we first analyzed the expression and intracellular distribution of β-catenin in the epidermis. We found an overall decrease of β-catenin protein levels in *Zmpste24*^{−/−} as compared with wild-type littermates (Fig. 4 A). Interestingly, no significant differences were found in the distribution of this protein in cells of the interfollicular epithelium or bulge region, whereas the intracellular accumulation of β-catenin in the hair bulb was observed in wild-type animals (Fig. 4 B). We reasoned that the observed cytoplasmic accumulation of β-catenin could represent a signaling-competent fraction of this protein. To test this hypothesis, we analyzed the expression and distribution of the active form of β-catenin (Act–β-catenin; van Noort et al., 2002). We found high levels of Act–β-catenin in the epidermis of wild-type animals but not in *Zmpste24*^{−/−} mice (Fig. 4 A). Similarly, a strong intracellular accumulation of Act–β-catenin was found in ∼30% of hair follicles in *Zmpste24*^{+/+} mice (Fig. 4 C). These results agree with the previously reported signaling capacity of β-catenin in this region during hair follicle development but not in the bulge, where Wnt signaling is thought to be constitutively inhibited (Blanpain and Fuchs, 2006). In contrast, <1% of hair follicles from *Zmpste24*^{−/−} animals contained nuclear β-catenin–positive cells in the hair bulb (Fig. 4 B). Notably, all changes in the expression and distribution patterns of β-catenin observed in the hair follicles of *Zmpste24*^{−/−} mice were restored in *Zmpste24*^{−/−} *Lmna*^{+/−} animals (Fig. 4 A and Fig. S3, A–C; available at http://www.jcb.org/cgi/content/full/jcb.200801096/DC1). In agreement with these observations, we found that the expression of cyclin D1, a direct proliferative target of the Wnt–β-catenin pathway (Tetsu and McCormick, 1999), was significantly reduced
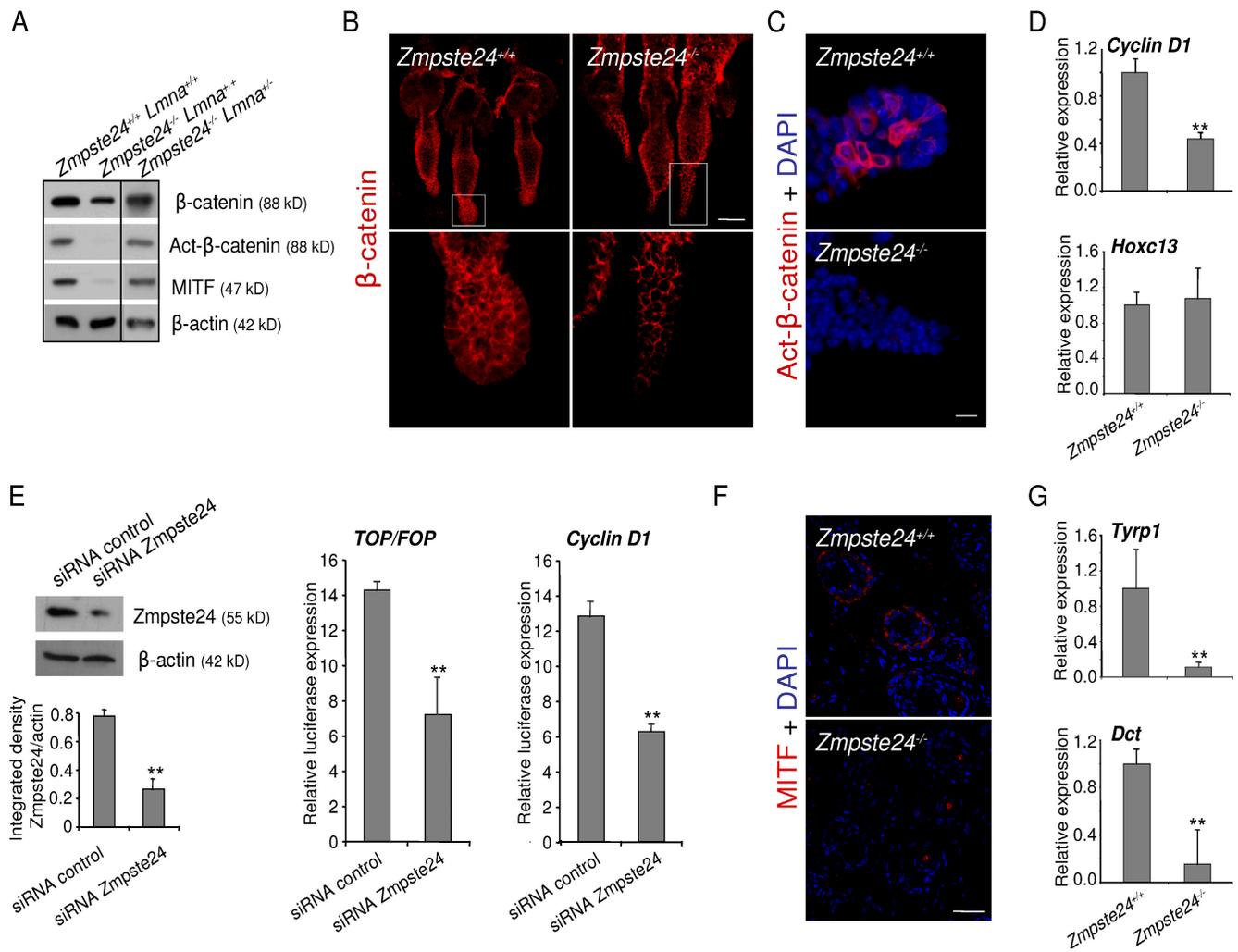
Figure 4. ***Zmpste24* deficiency disrupts signaling pathways implicated in stem cell regulation in the hair follicle.** (A) Immunoblot analysis of levels of β-catenin, active β-catenin, and Mitf in the epidermis of the indicated mice. β-Actin was analyzed as a loading control. Results are representative of three different animals per genotype. (B and C) Distribution of β-catenin and Act–β-catenin in tail skin hair follicles from *Zmpste24*$^{+/+}$ and *Zmpste24*$^{-/-}$ mice. (B) Boxed areas are magnified in the bottom panels. (D) Quantification of cyclin D1 and Hoxc13mRNA by quantitative RT-PCR. Data were normalized to *actin* expression. (E) RNAi experiments in Pam212 cells using Zmpste24-specific or scrambled siRNA. (left) Immunoblot analysis showing Zmpste24 protein reduction after 72 h of siRNA treatment. Results are representative of three experiments. (middle and right) Normalized luciferase/renilla activities of reporter vectors transiently transfected in Pam212 cells containing either multimerized promoter sequences recognized by β-catenin–lef/tcf complexes (pTOPFLASH; TOP), the same mutated sequences (pFOPFLASH; FOP), or the human cyclin D1 promoter. Assays were performed in triplicate. (F) Distribution of Mitf in the skin from *Zmpste24*$^{+/+}$ and *Zmpste24*$^{-/-}$ mice. (G) Quantification of mRNA expression by quantitative RT-PCR of dopachrome tautomerase and Tyrp1. **, P < 0.01. Error bars represent SEM. Bars: (B) 100 μm; (C) 20 μm; (F) 50 μm.

in the epidermis of *Zmpste24*$^{-/-}$ animals (Fig. 4 D). Likewise, we found that the activation of Akt and mTOR, two central transducers of the PI3K–Akt signaling pathway that modulate Wnt signaling in stem cells (Tian et al., 2005), was also repressed in the hair follicle of *Zmpste24*-null mice (Fig. S3 D).

To further investigate the causal role of pre–lamin A accumulation in the Wnt signaling dysfunction observed in *Zmpste24*$^{-/-}$ mice, we performed a series of gene reporter assays in Pam212 mouse keratinocytes. To this end, the transcriptional activity of constructs containing multimerized wild-type and mutated β-catenin/Lef1-binding sites or the mouse *cyclin D1* gene promoter fused to the luciferase reporter gene was analyzed in these cells after reducing their Zmpste24 levels by RNAi (Fig. 4 E). As can be seen in Fig. 4 E, both β-catenin–dependent and *cyclin D1* promoter transcription were efficiently inhibited in

Pam212 cells treated with specific siRNA directed to *Zmpste24* mRNA as compared with cells treated with control scrambled siRNA (Fig. 4 E). Therefore, according to these results, we can conclude that Wnt signaling is down-regulated by Zmpste24 depletion and can be altered in the stem cell–supporting epidermal hair bulb compartment of *Zmpste24*$^{-/-}$ mice. These findings are also of interest in the context of a recent study describing hyperactive Wnt signaling in a mouse model of accelerated aging caused by a mutation of Klotho (Liu et al., 2007). Despite the apparent divergence between our study and that of Liu et al. (2007), it must be emphasized that Klotho mice present hyperactive Wnt and a reduced number of bulge stem cells, whereas we have observed reduced Wnt signaling associated with stem cell accumulation in *Zmpste24*$^{-/-}$ animals, thus establishing a putative connection between both models.

Finally, we tested whether signaling pathways involved in the proliferation and differentiation of other stem cells present in the bulge yet distinct from epithelial stem cells could also be altered in *Zmpste24*$^{-/-}$ mice. For this purpose, we examined the protein levels of the microphthalmia transcription factor (Mitf), a master regulator of melanocyte stem cells that interacts with β-catenin to determine target gene expression (Nishimura et al., 2002; Schepsky et al., 2006). As seen in Fig. 4 A, very low levels of this transcription factor are present in the epidermis of *Zmpste24*$^{-/-}$ mice when compared with controls. Levels of Mitf expression were recovered in *Zmpste24*$^{-/-}$ *Lmna*$^{+/-}$ animals (Fig. 4 A). Immunofluorescence analysis also revealed the strong reduction of Mitf levels in hair follicles from *Zmpste24*$^{-/-}$ animals (Fig. 4 F). To further examine the loss of Mitf signaling in *Zmpste24*-null mice, we analyzed the expression of dopachrome tautomerase and tyrosinase-related protein 1 (Tyrp1), which are central effectors of Mitf in the bulge region (Nishimura et al., 2002). As shown in Fig. 4 G, we found that both Mitf effectors were severely down-regulated in *Zmpste24*$^{-/-}$ animals. From these results, we conclude that defective signaling of molecular circuits implicated in the functional regulation of epidermal (Wnt) or melanocyte (Mitf) stem cell activity in the skin occurs in *Zmpste24*-deficient mice. Remarkably, levels of the regulatory homeoprotein Hoxc13, which plays essential roles in hair follicle differentiation (Godwin and Capecchi, 1998), were maintained in *Zmpste24*$^{-/-}$ mice (Fig. 4 D), ruling out the occurrence of a general defect in this compartment that could affect all signaling pathways.

In summary, the results presented in this study are consistent with the proposal that the defects in nuclear architecture originally associated with progeroid syndromes in both mice and human have a strong impact on stem cells. By using mice deficient in specific components of the lamin A/Zmpste24 system, we have found that their stem cells accumulate in the hair follicle mainly as a result of defects in their proliferative potential. These deficiencies are linked to profound chromatin abnormalities as well as to the subsequent loss of signaling pathways, such as Wnt and Mitf, which play important roles in the regulation of stem cell number, fate, and function. These findings, together with the recent observation that nuclear envelope abnormalities could also be a central cause of normal aging (Haithcock et al., 2005; Scaffidi and Misteli, 2006), emphasize the relevance of progeria models to gain new insights into the connections between stem cell dysfunction and aging. These results also provide experimental support to the proposal that adult stem cell abnormalities may also influence the development of other laminopathies caused by defects in the nuclear envelope (Hutchison and Worman, 2004; Gotzmann and Foisner, 2006). In this regard, it is also interesting that *Lmna* is one of the genes markedly down-regulated in aged hematopoietic stem cells (Chambers et al., 2007), reinforcing the proposed importance of nuclear envelope alterations for stem cell dysregulation during aging. Finally, the observation that stem cell defects in *Zmpste24*$^{-/-}$ progeroid mice can be rescued in *Zmpste24*$^{-/-}$ *Lmna*$^{+/-}$ mice provides evidence for the causal relationship between nuclear lamina defects and stem cell dysfunction and opens the possibility of exploring new therapeutic approaches for human progeroid syndromes.

Materials and methods

Animals
Zmpste24$^{-/-}$ and *Zmpste24*$^{-/-}$ *Lmna*$^{+/-}$ mice were generated and genotyped as described previously (Pendás et al., 2002; Varela et al., 2005). To induce LRC mobilization, interfollicular epithelium hyperplasia, and anagen entry, tail skin from a group of six 75-d-old mice per genotype in the telogen (resting) phase of the hair cycle was topically treated every 48 h with TPA (20 nmol in acetone) for a total of three doses. Six control mice of each genotype were treated with acetone alone. 24 h after the last TPA treatment, mice were killed, and the tail skin was analyzed. Animal experimentation was performed in accordance with the guidelines of the Universidad de Oviedo.

Cultured keratinocytes, RNAi, and gene reporter assays
Pam212 is an immortalized and spontaneously transformed cell line from a BALB/c primary keratinocyte culture. Cells were grown in DME containing 10% (vol/vol) FCS, 50 U/ml penicillin, 50 μg/ml streptomycin, and 1% (vol/vol) of 0.2 M L-glutamine (all were obtained from Invitrogen). For *Zmpste24* RNAi, early subconfluent Pam212 cells were repeatedly transfected for 72 h with 100 nM of a validated siRNA duplex targeting *Zmpste24* mRNA (QIAGEN). Transfections were performed every 24 h using Oligofectamine (Invitrogen) in OptiMEM (Invitrogen) culture medium according to the manufacturer's instructions. For gene reporter assays, late subconfluent cells were transfected in duplicate in T-24 plates with 200 ng pTK-Renilla (Promega) and 400 ng of either pTOPFLASH or pFOPFLASH containing multimerized wild-type and mutated β-catenin/Lef1-binding sites, respectively (a gift from H. Clevers, Netherlands Institute for Developmental Biology, Utrecht, Netherlands), or the mouse *cyclin D1* promoter (a gift from A. Muñoz, Instituto de Investigaciones Biomedicas, Madrid, Spain) fused to the luciferase reporter gene. 600 ng of activator plasmid was added in each case as indicated. Activator plasmids included pCI-Lef1 (provided by H. Clevers) and pCI-mut-β-cat encoding a metabolically stabilized β-catenin S33Y (a gift from A. Ben-Ze'ev, Weizmann Institute of Science, Rehovot, Israel). Transfections were performed with Lipofectamine reagent (Invitrogen). DNA quantities were normalized with empty pcDNA3. Luciferase and Renilla activities were measured 24 h after transfection using the Dual Luciferase Reporter kit (Promega).

BrdU labeling of cells
BrdU LRCs were detected as previously described (Braun et al., 2003). In brief, mice were injected with 50 mg/kg body weight BrdU (Sigma-Aldrich) diluted in PBS. Each animal received a daily injection beginning at day 4 of life for a total of 5 d. After the labeling period, mice were allowed to grow for 60 d before the initiation of any treatment. Cells retaining the label at the end of the treatment were identified as LRCs. For short-term labeling, mice were treated daily beginning 4 d before being killed.

Histology and preparation of whole mounts
Tissue samples were harvested from mice, fixed overnight in neutral-buffered formalin, dehydrated through graded alcohols and xylene, and embedded in paraffin. Whole mounts of mouse tail epidermis were prepared as described previously (Braun et al., 2003). In brief, after mice were killed and tails were clipped, skin was peeled from the tails and incubated in 5 mM EDTA in PBS at 37°C for 4 h. Using forceps, intact sheets of epidermis were separated from the dermis and fixed in neutral-buffered formalin for 2 h at room temperature. Fixed epidermal sheets were maintained in PBS containing 0.2% sodium azide at 4°C before labeling.

Immunological methods
For immunofluorescence analysis of paraffin sections, slides were deparaffinized and rehydrated. When required, antigen retrieval was performed at 95°C for 40 min in 10 mM citrate containing 0.5% Triton X-100. Slides were washed in water, blocked in 5% BSA (Sigma-Aldrich) for 10 min, incubated with primary antibodies for 1 h at 37°C, washed in PBS, incubated for 40 min with secondary antibodies, thoroughly washed in water, and mounted in Vectashield (Vector Laboratories) containing DAPI for nuclear staining. For histology analysis, deparaffinized sections were stained with hematoxylin and eosin. For immunofluorescence of tail skin whole mounts, epidermal sheets were blocked and permeabilized in PBS containing 0.5% gelatin and 0.5% Triton X-100 (PGT) for 30 min and incubated with primary antibodies diluted in PGT overnight at 37°C. Samples were washed in PGT for 1 h, incubated for 2 h with secondary antibodies, washed 1 h in PGT, cleared in water, and mounted in Vectashield. Protein extracts for immunoblot analysis were obtained in NT buffer (50 mM Tris-HCl, pH 7.4, 100 mM

NaCl, 5 mM MgCl$_2$, 5 mM CaCl$_2$, 1% NP-40, and 1% Triton X-100) containing protease and phosphatase inhibitors (2 mM PMSF, 20 µg/ml aprotinin, and 1 mM sodium orthovanadate; all were obtained from Sigma-Aldrich). Mouse monoclonal against 5mC was provided by M. Esteller (Spanish National Cancer Research Center, Madrid, Spain). Goat polyclonal antibodies against lamin A/C and pre–lamin A were purchased from Santa Cruz Biotechnology, Inc. Mouse monoclonal anti-active β-catenin (clone 8E7) was obtained from Millipore. Mouse monoclonal against β-catenin (clone 14) was purchased from Transduction Laboratories. Mouse monoclonal antibodies against cytokeratin 15, Mitf, and HP1α and rabbit polyclonals against cytokeratin 19, Ki67, α6-integrin, and trimethylated histone H3 (Lys9) were purchased from Abcam. Mouse monoclonal antibody against phospho-Akt (Ser473; clone 587F11) and rabbit monoclonal against phospho-mTOR (Ser2448; clone 49F9) were obtained from Cell Signaling Technology. Secondary antibodies included Cy2, Cy3, peroxidase-conjugated goat antibodies to mouse or rabbit IgG Fab fragments, and Cy3 and peroxidase-conjugated donkey antibodies to goat IgG Fab fragments (Jackson ImmunoResearch Laboratories). To detect BrdU LRCs or BrdU short-term labeled samples, paraffin sections or whole mounts were blocked and permeabilized by incubation in PGT for 30 min. Subsequently, samples were treated for 30 min with 2 M HCl at 37°C, incubated overnight with a mouse anti-BrdU antibody conjugated with fluorescein (Roche) at 1:50 in PGT buffer, washed in PGT, and mounted in Vectashield. Apoptotic cells were identified after fluorescent TUNEL labeling as recommended by the manufacturer (Roche). Images of immunolabeled samples were obtained at room temperature with a laser-scanning confocal microscope (TCS-SP2-AOBS; Leica) using HC PL APO CS 20× NA 0.70, HCX PL APO CS 40× NA 1.25, and HCX PL APO lbd BL 63× NA 1.4 objective lenses. Images were acquired with LCS Suite version 2.61 (Leica), and the brightness/contrast was adjusted with Photoshop CS version 9.0.2 (Adobe).

Isolation of keratinocytes and clonogenic assays

2- and 75-d-old mice were killed and successively soaked in betadine for 5 min, PBS antibiotics solution for 5 min, 70% ethanol for 5 min, and PBS antibiotics solution for 5 min. Limbs and tail from newborn mice were clipped, and the remaining skin was peeled off using forceps, whereas in the case of adult mice, skin from the entire tail was collected. In both cases, collected skin samples were then soaked in PBS for 2 min, PBS antibiotics solution for 2 min, 70% ethanol for 1 min, and PBS antibiotics solution for 2 min. Using forceps, each skin was floated on the surface of 4 ml trypsin solution on a 60-mm cell culture plate for 16 h at 4°C or for 3 h at 37°C (in the case of adult keratinocytes). Skins were transferred to a sterile surface, and the epidermis was separated from the dermis using forceps and was minced and stirred at 37°C for 30 min in serum-free Cnt-02 medium (CELLnTEC Advanced Cell Systems). The cell suspension was filtered through a sterile Teflon mesh (Cell Strainer; Falcon) to remove cornified sheets. Keratinocytes were then collected by centrifugation at 160 g for 10 min and counted. 1,000 keratinocytes obtained from 2-d-old mice and 10^4 keratinocytes from 2-mo-old mice were seeded onto mitomycin C (10 µg/ml; 2 h)-treated J2-3T3 fibroblasts (10^5 per well; six-well dishes) and grown at 37°C and 5% CO$_2$ in Cnt-02 medium. After 10 d of culture, dishes were rinsed twice with PBS, fixed in 10% formaldehyde, and stained with 1% rhodamine B to visualize colony formation. Colony size and number were measured using three dishes per experiment over a total of three separate experiments. To induce differentiation, 1.5 mM calcium was added to Cnt-02 medium.

Real-time quantitative PCR

Expression levels of selected genes were analyzed by using Taqman gene expression assays (Applied Biosystems) in a sequence detection system (ABI7000; Applied Biosystems) according to the manufacturer's instructions.

Statistical analysis

Statistical analysis of differences between mouse cohorts was performed using the t test. Excel (Microsoft) was used for calculations, and results were expressed as the mean ± SEM.

Online supplemental material

Fig. S1 shows the enrichment of cytokeratin 19 in the bulge region of Zmpste24$^{-/-}$ mice. Fig. S2 shows alterations in the distribution of heterochromatin markers in the hair bulb and interfollicular epithelium of Zmpste24$^{-/-}$ mice and the absence of qualitative changes in the differentiation potential of stem cells from these mice. Fig. S3 shows the rescue of Zmpste24$^{-/-}$ stem cell dysfunction in Zmpste24$^{-/-}$ Lmna$^{+/-}$ mice and the occurrence of PI3K–Akt pathway alterations in the hair follicle of Zmpste24$^{-/-}$

mice. Online supplemental material is available at http://www.jcb.org/cgi/content/full/jcb.200801096/DC1.

References

Blanpain, C., and E. Fuchs. 2006. Epidermal stem cells of the skin. *Annu. Rev. Cell Dev. Biol.* 22:339–373.

Braun, K.M., C. Niemann, U.B. Jensen, J.P. Sundberg, V. Silva-Vargas, and F.M. Watt. 2003. Manipulation of stem cell proliferation and lineage commitment: visualisation of label-retaining cells in wholemounts of mouse epidermis. *Development.* 130:5241–5255.

Broers, J.L., F.C. Ramaekers, G. Bonne, R.B. Yaou, and C.J. Hutchison. 2006. Nuclear lamins: laminopathies and their role in premature ageing. *Physiol. Rev.* 86:967–1008.

Cadiñanos, J., I. Varela, C. López-Otín, and J.M. Freije. 2005. From immature lamin to premature aging: molecular pathways and therapeutic opportunities. *Cell Cycle.* 4:1732–1735.

Campisi, J. 2005. Senescent cells, tumor suppression, and organismal aging: good citizens, bad neighbors. *Cell.* 120:513–522.

Capell, B.C., and F.S. Collins. 2006. Human laminopathies: nuclei gone genetically awry. *Nat. Rev. Genet.* 7:940–952.

Chambers, S.M., C.A. Shaw, C. Gatza, C.J. Fisk, L.A. Donehower, and M.A. Goodell. 2007. Aging hematopoietic stem cells decline in function and exhibit epigenetic dysregulation. *PLoS Biol.* 5:e201.

Clevers, H. 2006. Wnt/beta-catenin signaling in development and disease. *Cell.* 127:469–480.

Cotsarelis, G., T.T. Sun, and R.M. Lavker. 1990. Label-retaining cells reside in the bulge area of pilosebaceous unit: implications for follicular stem cells, hair cycle, and skin carcinogenesis. *Cell.* 61:1329–1337.

Filesi, I., F. Gullotta, G. Lattanzi, M.R. D'Apice, C. Capanni, A.M. Nardone, M. Columbaro, G. Scarano, E. Mattioli, P. Sabatelli, et al. 2005. Alterations of nuclear envelope and chromatin organization in mandibuloacral dysplasia, a rare form of laminopathy. *Physiol. Genomics.* 23:150–158.

Flores, I., M.L. Cayuela, and M.A. Blasco. 2005. Effects of telomerase and telomere length on epidermal stem cell behavior. *Science.* 309:1253–1256.

Fong, L.G., J.K. Ng, M. Meta, N. Cote, S.H. Yang, C.L. Stewart, T. Sullivan, A. Burghardt, S. Majumdar, K. Reue, et al. 2004. Heterozygosity for Lmna deficiency eliminates the progeria-like phenotypes in Zmpste24-deficient mice. *Proc. Natl. Acad. Sci. USA.* 101:18111–18116.

Godwin, A.R., and M.R. Capecchi. 1998. Hoxc13 mutant mice lack external hair. *Genes Dev.* 12:11–20.

Gotzmann, J., and R. Foisner. 2006. A-type lamin complexes and regenerative potential: a step towards understanding laminopathic diseases? *Histochem. Cell Biol.* 125:33–41.

Haithcock, E., Y. Dayani, E. Neufeld, A.J. Zahand, N. Feinstein, A. Mattout, Y. Gruenbaum, and J. Liu. 2005. Age-related changes of nuclear architecture in *Caenorhabditis elegans. Proc. Natl. Acad. Sci. USA.* 102:16690–16695.

Hasty, P., J. Campisi, J. Hoeijmakers, H. van Steeg, and J. Vijg. 2003. Aging and genome maintenance: lessons from the mouse? *Science.* 299:1355–1359.

Howard, B.H. 1996. Replicative senescence: considerations relating to the stability of heterochromatin domains. *Exp. Gerontol.* 31:281–293.

Hutchison, C.J., and H.J. Worman. 2004. A-type lamins: guardians of the soma? *Nat. Cell Biol.* 6:1062–1067.

Jones, D.L., and A.J. Wagers. 2008. No place like home: anatomy and function of the stem cell niche. *Nat. Rev. Mol. Cell Biol.* 9:11–21.

Kipling, D., T. Davis, E.L. Ostler, and R.G. Faragher. 2004. What can progeroid syndromes tell us about human aging? *Science.* 305:1426–1431.

Kirkwood, T.B. 2005. Understanding the odd science of aging. *Cell.* 120:437–447.

Liu, H., M.M. Fergusson, R.M. Castilho, J. Liu, L. Cao, J. Chen, D. Malide, I.I. Rovira, D. Schimel, C.J. Kuo, et al. 2007. Augmented Wnt signaling in a mammalian model of accelerated aging. *Science.* 317:803–806.

Liu, Y., S. Lyle, Z. Yang, and G. Cotsarelis. 2003. Keratin 15 promoter targets putative epithelial stem cells in the hair follicle bulge. *J. Invest. Dermatol.* 121:963–968.

Lo Celso, C., D.M. Prowse, and F.M. Watt. 2004. Transient activation of beta-catenin signalling in adult mouse epidermis is sufficient to induce new hair follicles but continuous activation is required to maintain hair follicle tumours. *Development.* 131:1787–1799.

Navarro, C.L., P. Cau, and N. Levy. 2006. Molecular bases of progeroid syndromes. *Hum. Mol. Genet.* 15 Spec No 2:R151–R161.

Nishimura, E.K., S.A. Jordan, H. Oshima, H. Yoshida, M. Osawa, M. Moriyama, I.J. Jackson, Y. Barrandon, Y. Miyachi, and S. Nishikawa. 2002. Dominant role of the niche in melanocyte stem-cell fate determination. *Nature.* 416:854–860.

Pendás, A.M., Z. Zhou, J. Cadiñanos, J.M. Freije, J. Wang, K. Hultenby, A. Astudillo, A. Wernerson, F. Rodríguez, K. Tryggvason, and C. López-Otín. 2002. Defective prelamin A processing and muscular and adipocyte alterations in Zmpste24 metalloproteinase-deficient mice. *Nat. Genet.* 31:94–99.

Ramírez, C.L., J. Cadiñanos, I. Varela, J. Freije, and C. Lopez-Otín. 2007. Human progeroid syndromes, aging and cancer: new genetic and epigenetic insights into old questions. *Cell. Mol. Life Sci.* 64:155–170.

Rando, T.A. 2006. Stem cells, ageing and the quest for immortality. *Nature.* 441:1080–1086.

Scaffidi, P., and T. Misteli. 2006. Lamin A-dependent nuclear defects in human aging. *Science.* 312:1059–1063.

Schepsky, A., K. Bruser, G.J. Gunnarsson, J. Goodall, J.H. Hallsson, C.R. Goding, E. Steingrimsson, and A. Hecht. 2006. The microphthalmia-associated transcription factor Mitf interacts with beta-catenin to determine target gene expression. *Mol. Cell. Biol.* 26:8914–8927.

Shumaker, D.K., T. Dechat, A. Kohlmaier, S.A. Adam, M.R. Bozovsky, M.R. Erdos, M. Eriksson, A.E. Goldman, S. Khuon, F.S. Collins, et al. 2006. Mutant nuclear lamin A leads to progressive alterations of epigenetic control in premature aging. *Proc. Natl. Acad. Sci. USA.* 103:8703–8708.

Tetsu, O., and F. McCormick. 1999. Beta-catenin regulates expression of cyclin D1 in colon carcinoma cells. *Nature.* 398:422–426.

Tian, Q., X.C. He, L. Hood, and L. Li. 2005. Bridging the BMP and Wnt pathways by PI3 kinase/Akt and 14-3-3zeta. *Cell Cycle.* 4:215–216.

van Noort, M., J. Meeldijk, R. van der Zee, O. Destree, and H. Clevers. 2002. Wnt signaling controls the phosphorylation status of beta-catenin. *J. Biol. Chem.* 277:17901–17905.

Varela, I., J. Cadiñanos, A.M. Pendás, A. Gutiérrez-Fernández, A.R. Folgueras, L.M. Sánchez, Z. Zhou, F.J. Rodríguez, C.L. Stewart, J.A. Vega, et al. 2005. Accelerated ageing in mice deficient in Zmpste24 protease is linked to p53 signalling activation. *Nature.* 437:564–568.